

A New Direction in Dark-Matter Complementarity: Dark-Matter Decay as a Complementary Probe of Multi-Component Dark Sectors

Keith R. Dienes^{1,2*}, Jason Kumar^{3†}, Brooks Thomas^{4‡}, David Yaylali^{3§}

¹ *Department of Physics, University of Arizona, Tucson, AZ 85721 USA*

² *Department of Physics, University of Maryland, College Park, MD 20742 USA*

³ *Department of Physics, University of Hawaii, Honolulu, HI 96822 USA*

⁴ *Department of Physics, Carleton University, Ottawa, ON K1S 5B6 Canada*

In single-component theories of dark matter, the $2 \rightarrow 2$ amplitudes for dark-matter production, annihilation, and scattering can be related to each other through various crossing symmetries. These crossing relations lie at the heart of the celebrated complementarity which underpins different existing dark-matter search techniques and strategies. In *multi-component* theories of dark matter, by contrast, there can be many different dark-matter components with differing masses. This then opens up a new, “diagonal” direction for dark-matter complementarity: the possibility of dark-matter *decay* from heavier to lighter dark-matter components. In this work, we discuss how this new direction may be correlated with the others, and demonstrate that the enhanced complementarity which emerges can be an important ingredient in probing and constraining the parameter spaces of such models.

Introduction.— In recent years, many search techniques have been exploited in the hunt for dark matter [1]. These include possible dark-matter production at colliders; direct detection of cosmological dark matter through its scattering off ordinary matter at underground experiments; and indirect detection of dark matter through observation of the remnants of the annihilation of cosmological dark matter into ordinary matter at terrestrial or satellite-based experiments. At first glance, these different techniques may seem to rely on three independent properties of dark matter, namely its amplitudes for production, scattering, and annihilation. However, these three amplitudes are often related to each other through various crossing symmetries. As a result, the different corresponding search techniques are actually correlated with each other through their dependence on a single underlying interaction which couples dark matter to ordinary matter, and the results achieved through any one of these search techniques will have immediate implications for the others as well as for this underlying interaction. This is the origin of the celebrated complementarity which connects the different existing dark-matter search techniques (for a review, see Ref. [2]).

Most studies of this complementarity implicitly assume that the dark sector consists of a single particle χ . Indeed, many studies further focus on a particular effective $2 \rightarrow 2$ interaction between dark matter and ordinary matter, as sketched in Fig. 1(a); the three complementary search strategies then correspond to physical processes in which we imagine time flowing in the directions associated with the three different blue arrows.

Indeed, because of the assumed single-particle nature of the dark sector, we further observe that the scattering that underlies direct-detection experiments is necessarily elastic. Likewise, the dark-matter-induced production of ordinary matter that underlies indirect-detection experiments exclusively takes place through annihilation of the dark-matter particle with itself or its antiparticle.

In this paper, we point out that this situation becomes far richer in *multi-component* theories of dark matter. In particular, if we assume that the dark sector consists of at least two different dark-matter components χ_i and χ_j with differing masses $m_i \neq m_j$, then for $i \neq j$ the situation differs from the single-particle case in two fundamental ways. First, the kinematics associated with each of the traditional complementarity directions is altered: dark-matter production becomes *asymmetric* rather than symmetric; dark-matter annihilation of one dark particle against itself or its antiparticle becomes *co-annihilation* between two different dark species; and dark-matter scattering — previously exclusively elastic — now becomes *inelastic*, taking the form of either “up-scattering” [3] or “down-scattering” [4] depending on whether it is the incoming or outgoing dark-matter particle which has greater mass. These kinematic changes are illustrated in Fig. 1(b), and can significantly affect the phenomenology of the corresponding processes. But perhaps even more importantly, an entirely new direction for dark-matter complementarity also opens up: this is the possibility of dark-matter *decay* from heavier to lighter dark-matter components. Indeed, this process corresponds to the *diagonal* direction for the imagined flow of time, as shown in Fig. 1(b), and thus represents an entirely new direction for dark-matter complementarity. Such a direction was not available in single-component theories of dark matter due to phase-space constraints, and is ultimately driven by the non-zero mass difference between the associated parent and daughter dark-matter particles. Of course,

*E-mail address: dienes@email.arizona.edu

†E-mail address: jkumar@hawaii.edu

‡E-mail address: bthomas@physics.carleton.ca

§E-mail address: yaylali@hawaii.edu

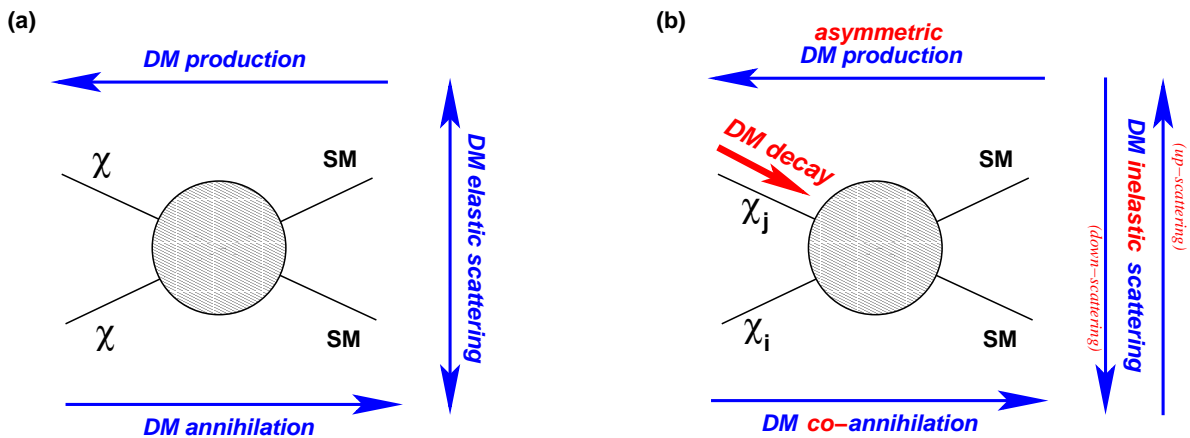


FIG. 1: (a) In single-component theories of dark matter, the $2 \rightarrow 2$ amplitudes for dark-matter production, annihilation, and scattering are related to each other through various crossing symmetries. These different processes correspond to different directions (blue arrows) for the imagined flow of time through a single four-point diagram. (b) In *multi-component* theories of dark matter, by contrast, there can be many different dark-matter components χ_i with differing masses m_i . Taking $m_i \neq m_j$ then changes the kinematics associated with each of the previous complementary directions: dark-matter production becomes *asymmetric* rather than symmetric; dark-matter annihilation of one dark particle against itself becomes *co-annihilation* between two different dark species; and elastic dark-matter scattering becomes *inelastic*, taking the form of either “down-scattering” or “up-scattering” depending on whether it is the incoming or outgoing dark-matter particle which has greater mass. Even more importantly, however, the existence of a non-minimal dark sector opens up the possibility for an additional process which is also related the others by crossing symmetries: dark-matter *decay* from heavier to lighter dark-matter components. This process corresponds to a *diagonal* direction for the imagined flow of time, as shown, and thus represents a new direction for dark-matter complementarity.

we are not the first to discuss decaying dark matter of this form (see, *e.g.*, Refs. [4–6] for prior work). However our main point is that these decays are actually part of a larger complementarity, and that this enhanced complementarity can be an important ingredient in probing and constraining the parameter spaces of theories with non-trivial dark sectors.

Thus, if the dark sector consists of multiple components, a generic four-point interaction of the sort shown in Fig. 1 will lead to an enhanced set of complementarities across different classes of dark-matter experiments. Direct-detection experiments will potentially be sensitive to nuclear recoils from elastic scattering, up-scattering, and down-scattering, while indirect-detection experiments will potentially be able to measure fluxes from dark-matter self-annihilation, dark-matter co-annihilation, and dark-matter decay. Likewise, collider experiments will potentially involve dark-matter production which is both symmetric and asymmetric. Of course, neither inelastic down-scattering nor dark-matter decay will be relevant for present-day experiments unless the more massive dark-matter components have significant cosmological abundances at the present time; indeed, this already places one set of constraints on their decay widths. In this connection, we also note that this same four-point interaction can in principle also give rise to an additional process in which a heavy ordinary-matter particle

decays into a lighter ordinary-matter particle along with two dark-sector particles. However, for all cases involving two quarks (which will be our main interest in this paper), such processes cannot occur in a flavor-conserving theory. Processes of this type will therefore not be considered further in this paper. We nevertheless note that in general, exotic decays of the Higgs or of Standard-Model electroweak gauge bosons could potentially provide yet another complementary probe into the nature of the dark sector [6].

Two Examples.— In order to illustrate these extra complementarities and the power they provide in surveying the parameter space of theories with multi-component dark sectors, let us imagine that the dark sector consists of two Dirac fermions χ_1 and χ_2 which are neutral under all Standard-Model gauge symmetries and have corresponding masses m_1 and m_2 respectively, with $m_2 > m_1$. We shall also assume that our fundamental four-point interaction in Fig. 1(b) is described by an effective dimension-six four-fermi contact Lagrangian operator that couples these two dark-matter particles to two Standard-Model quarks q . For concreteness, in this paper we shall consider two distinct examples of such operators, with the first taking the form of a flavor-conserving scalar (S) interaction

$$\mathcal{L}_{\text{int}}^{(S)} = \sum_{q=u,d,s,\dots} \frac{c_q^{(S)}}{\Lambda^2} (\bar{\chi}_2 \chi_1) (\bar{q} q) + \text{h.c.}, \quad (1)$$

and the second taking the form of a flavor-conserving

axial-vector (A) interaction

$$\mathcal{L}_{\text{int}}^{(A)} = \sum_{q=u,d,s,\dots} \frac{c_q^{(A)}}{\Lambda^2} (\bar{\chi}_2 \gamma_\mu \gamma^5 \chi_1) (\bar{q} \gamma^\mu \gamma^5 q) + \text{h.c.} \quad (2)$$

We have chosen these two forms of interactions as canonical examples of operators giving rise to spin-independent (SI) and spin-dependent (SD) interactions, respectively. In these operators, $q = u, d, s, \dots$ specifies a particular quark flavor while c_q is the corresponding dark-matter/quark coupling and Λ denotes the mass scale of the new (presumably flavor-diagonal) physics which might generate such effective interactions. Note that these operators are separately invariant under both charge conjugation (C) and parity (P). Of course, the scalar operator structure explicitly violates the chiral symmetries of the Standard Model. The coefficient of this operator thus implicitly includes a vev of the Higgs field, so that we would in this case more precisely identify $\Lambda' \equiv (\Lambda^2 v)^{1/3}$ as the scale of new physics.

Within the operators in Eqs. (1) and (2), we shall make two further assumptions. First, in each case, we shall assume a flavor structure for our dark-matter/quark couplings c_q such that

$$c_u = -c_d = c_c = -c_s = c_t = -c_b \equiv c. \quad (3)$$

We have chosen this flavor structure, which is maximally isospin-violating within each generation, because it ultimately maximizes the axial-vector decay rate and thereby places the strongest bounds on our examples. Second, we shall assume (as a cosmological input) that the heavier dark-matter particle χ_2 is metastable and carries the vast majority of the dark-matter abundance, *i.e.*, $\Omega_2 = \Omega_{\text{CDM}} \approx 0.26$ and $\Omega_1 = 0$. As we shall see, this assumption also maximizes the rates for all relevant processes and thereby places the strongest bounds on our examples. This assumption also simplifies our analysis somewhat. We shall therefore take this to be a conservative “benchmark” for our study. We remark, however, that none of the primary qualitative aspects of our results will ultimately depend on this choice, and indeed other choices such as $\Omega_1 \approx \Omega_2 \approx \Omega_{\text{CDM}}/2$ also lead to results which are very similar to those we shall obtain here. Such general scenarios will be explored in Ref. [7].

Given these assumptions, our examples each have three fundamental parameters: the effective coupling c/Λ^2 , the mass m_2 of the heavier dark-matter component, and the dark-sector mass splitting $\Delta m_{12} \equiv m_2 - m_1$. Our goal is to explore the resulting $(c/\Lambda^2, \Delta m_{12})$ parameter space for different values of m_2 . In this connection, however, we remark that since the operators in Eqs. (1) and (2) are non-renormalizable, they can only be interpreted within the context of an effective field theory whose cut-off scale is parametrically connected to Λ . As a result, our use of such operators when calculating phenomenological bounds already presupposes that the energy scales

associated with the relevant processes in each case do not exceed Λ . Assuming $\mathcal{O}(1)$ operator coefficients, this requires $\Lambda \gtrsim \mathcal{O}(\text{GeV})$ for direct-detection bounds; indeed, as we shall see, this value corresponds to nuclear recoil energies $E_R \lesssim 100$ keV in direct-detection experiments. Likewise, for indirect-detection bounds, our requirement for Λ depends on whether we are dealing with dark-matter annihilation or decay: for annihilation this requires $\Lambda \gtrsim \mathcal{O}(m)$ where m is a typical mass of a dark-sector component, while for a dark-matter decay of the form $\chi_2 \rightarrow \chi_1 \bar{q} q$ this requires $\Lambda \gtrsim \mathcal{O}(\Delta m_{12})$. Finally, for calculating collider-production bounds, the use of such operators is strictly valid only if $\Lambda \gtrsim \mathcal{O}(\text{TeV})$. If this last condition is not met, the resulting collider bounds should be viewed only as heuristic, and one would require a more complete theory (for example, involving potentially light mediators connecting the dark and visible sectors) before being able to make more precise statements.

As $\Delta m_{12} \rightarrow 0$, our dark-matter production and direct-detection processes proceed exactly as they would for a single dark-matter particle χ of mass $m = m_2$. Indeed, in this limit direct detection can only proceed through elastic scattering; likewise, the interactions in Eq. (1) or (2) do not permit dark-matter decay. Thus, the $\Delta m_{12} \rightarrow 0$ limit effectively embodies the physics of a traditional single-component dark sector with mass m_2 , and in this case our bounds are relatively straightforward: one simply finds that direct-detection and collider experiments place m_2 -dependent upper limits on the coupling c/Λ^2 . For example, for the coupling structure in Eq. (3) and for $m_2 = 100$ GeV, we find from direct-detection experiments [8, 9] that

$$\begin{cases} c^{(S)}/\Lambda^2 \lesssim 2.8 \times 10^{-10} \text{ GeV}^{-2}, \\ c^{(A)}/\Lambda^2 \lesssim 1.1 \times 10^{-5} \text{ GeV}^{-2}; \end{cases} \quad (4)$$

we likewise find from collider monojet [10, 11] and mono- W/Z [12] constraints that

$$\begin{cases} c^{(S,A)}/\Lambda^2 \lesssim 1.4 \times 10^{-6} \text{ GeV}^{-2} \text{ (monojet)}, \\ c^{(S)}/\Lambda^2 \lesssim 5.0 \times 10^{-7} \text{ GeV}^{-2} \text{ (mono-}W/Z), \\ c^{(A)}/\Lambda^2 \lesssim 3.1 \times 10^{-7} \text{ GeV}^{-2} \text{ (mono-}W/Z). \end{cases} \quad (5)$$

However, by turning on Δm_{12} , we can now explore the effects of non-minimality in the dark sector and thereby assess the impact of the new kinematics and new complementarities that arise.

With an eye towards exploring those regions of parameter space which are likely to be of maximal phenomenological interest from a complementarity perspective, we shall restrict our attention to situations with $\Delta m_{12} \lesssim \mathcal{O}(\text{MeV})$; we stress, however, that there is no fundamental reason that larger Δm_{12} cannot also be considered. Note that a small mass splitting $\Delta m_{12} \ll m_1, m_2$ can be realized naturally in models wherein the generation of Δm_{12} is associated with the breaking of an

approximate symmetry (see, *e.g.*, Ref. [3]). Examples include models in which a Dirac fermion is split into a pair of nearly degenerate Majorana states by a small Majorana mass, and models in which a complex scalar is split into two real scalars by a small holomorphic mass.

Since we are taking $\Omega_1 = 0$ for simplicity, the relevant dark-matter processes for the operators in Eqs. (1) and (2) are limited to inelastic down-scattering, asymmetric collider production, and dark-matter decay. We shall now discuss each of these in turn.

Inelastic down-scattering.— We begin by considering the bounds from direct-detection experiments through the inelastic down-scattering process $\chi_2 N_i \rightarrow \chi_1 N_f$ where N_i and N_f denote the initial and final states of the nucleus N in the detector substrate. In general, the total differential nuclear-recoil rate is given by

$$\frac{dR}{dE_R} = \frac{\tilde{N} \rho_2^{\text{loc}}}{m_2} \int_{v > v_{\min}^{(21)}} v \mathcal{F}_2(\vec{v}) \left(\frac{d\sigma_{21}}{dE_R} \right) d^3v, \quad (6)$$

where \tilde{N} is the number of nuclei per unit detector mass, where ρ_2^{loc} is the local energy density of χ_2 , where $\mathcal{F}_2(\vec{v})$ is the distribution of detector-frame velocities \vec{v} for χ_2 in the local dark-matter halo, where $v = |\vec{v}|$, where $v_{\min}^{(21)}$ is the E_R -dependent “threshold” velocity (*i.e.*, the minimum incoming velocity for which scattering with recoil energy E_R is possible), and where $d\sigma_{21}/dE_R$ is the differential cross-section for the process $\chi_2 N_i \rightarrow \chi_1 N_f$. When evaluating these cross-sections, we require nuclear form factors; for this purpose we utilize the software packages associated with Ref. [13]. The corresponding limits on our $(c/\Lambda^2, \Delta m_{12})$ parameter space are then respectively derived using the most recent LUX [8] and COUPP-4 [9] data for the scalar and axial-vector cases, respectively. Roughly speaking, this data can be taken as requiring $R \lesssim 1.81 \times 10^{-4} \text{ kg}^{-1} \text{ day}^{-1}$ and $R \lesssim 4.97 \times 10^{-2} \text{ kg}^{-1} \text{ day}^{-1}$ for the recoil-energy windows $3 \text{ keV} \leq E_R \leq 25 \text{ keV}$ and $7.8 \text{ keV} \leq E_R \leq 100 \text{ keV}$, respectively. In this connection, we note that a threshold detector such as COUPP-4 is actually sensitive to scattering events with arbitrarily large recoil energies. However, for $E_R \gtrsim 100 \text{ keV}$, there are considerable uncertainties associated with distinguishing these events from background. To be conservative, we therefore adopt the above upper limit for the corresponding E_R window.

While much of this analysis is completely standard, the primary new ingredient is the change in scattering kinematics from elastic to inelastic. If the scattering had been elastic (*e.g.*, $\chi_j N_i \rightarrow \chi_j N_f$), the possible allowed recoil energies would have been given by the standard expression $E_R = E_{jN}(1 + \cos\theta)$ where $E_{jN} \equiv \mu_{jN}^2 v_j^2 / m_N$ and $0 \leq \theta \leq \pi$. Here v_j is the speed of the incoming dark-matter particle in the detector frame, m_N the mass of the nucleus, θ the scattering angle in the center-of-mass frame, and $\mu_{\chi N}$ the reduced mass of the χ/N system. For inelastic $\chi_j N_i \rightarrow \chi_i N_f$ scattering, by contrast, the

possible allowed recoil energies are instead given by $E_R = E_{jN}(1 + r + \sqrt{1 + 2r \cos\theta})$ where $r \equiv [\mu_{iN}/(\beta\mu_{jN})^2] \Delta m_{ij}$ with $\beta \equiv v_j/c$ and $\Delta m_{ij} \equiv m_j - m_i$.

There are two important consequences of this change in kinematics. First, in the case of down-scattering, we see that for $E_R \approx E_R^* \equiv [m_i/(m_i + m_N)] \Delta m_{ij} c^2$ the required incoming velocity is essentially zero. Such threshold-free scattering with non-zero recoil energy would not have been possible in the traditional case of elastic scattering, but the required input energy in the inelastic case comes directly from species conversion within the dark sector (essentially from rest mass liberated within the dark sector) rather than from incoming dark-sector kinetic energy.

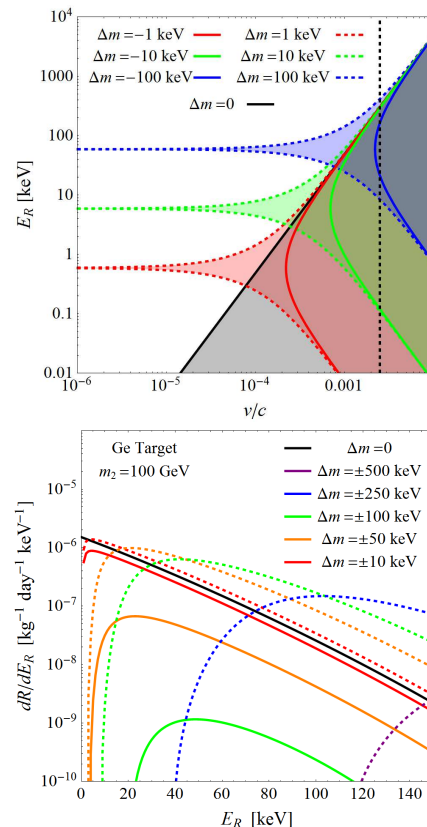


FIG. 2: Recoil-energy spectra for inelastic scattering $\chi_2 N_i \rightarrow \chi_1 N_f$ off a germanium nucleus, with $m_1 \neq m_2 = 100 \text{ GeV}$. *Top panel:* Allowed ranges of recoil energy E_R as a function of incoming dark-matter particle velocity v for different $\Delta m \equiv m_2 - m_1$, for both “down-scattering” ($\Delta m > 0$, dotted lines) and “up-scattering” ($\Delta m < 0$, solid lines). The elastic case with $\Delta m = 0$ is also shown (solid black line), as is the maximum velocity cutoff associated with the galactic escape velocity (dashed black line). *Bottom panel:* Corresponding recoil spectra dE_R/dR for both down-scattering (dotted lines) and up-scattering (solid lines), for different values of Δm . The solid black curve represents the $\Delta m = 0$ elastic-scattering case. For all spectra shown, the scattering is assumed to be spin-independent, with cross-section per nucleon $\sim 10^{-46} \text{ cm}^{-2}$.

Second, we also observe that for any incoming dark-matter velocity v , we have not only a finite upper limit on the allowed nuclear recoil energy E_R but also a non-zero *lower* limit. This feature holds for both down-scattering and up-scattering, and in turn implies that the corresponding recoil spectrum dR/dE_R is negligible not only above a maximum value of nuclear recoil energy *but also below a minimal value*. Indeed, in the case of down-scattering (*i.e.*, $\Delta m > 0$), this allowed range of recoil energies is centered around E_R^* and becomes exceedingly narrow as the incoming velocity goes to zero. This is especially important since $v \leq v_{\text{esc}} + v_E$, where $v_{\text{esc}} \approx 540$ km/s is the galactic escape velocity and $v_E \approx 231$ km/s is the speed of the Earth in the galactic frame. These features are illustrated in Fig. 2, and will play an important role in what follows.

Asymmetric collider production.— Multi-component operators such as those in Eqs. (1) and (2) can also be probed through the collider-production direction. However, unlike the single-component case, the production processes induced by the operators in Eqs. (1) and (2) take the form $qq \rightarrow \chi_1\chi_2$. Thus, we are dealing with *asymmetric* collider production of dark matter.

Despite this new feature, such dark-matter production processes can nevertheless be most effectively constrained just as for single-component theories — *i.e.*, through monojet searches at ATLAS [10] and CMS [11] and mono- W/Z searches at ATLAS [12]. Indeed, these limits are directly applicable to the asymmetric production of dark-matter particles χ_1 and χ_2 as well as to a pair of identical dark-matter particles because the values of Δm_{12} for which inelastic scattering can play a significant role in direct detection (and for which χ_2 is stable on cosmologically timescales without exceedingly large Λ) are negligibly small in comparison with the energy scales relevant for collider physics. Thus, while the kinematics associated with the asymmetric production of dark matter differs from that associated with the more traditional symmetric production, this difference ultimately does not prove phenomenologically significant within the parameter ranges of greatest interest from a complementarity perspective.

Dark-matter decay.— We now turn to an analysis of the new (diagonal) complementarity direction which comes into existence for non-zero Δm_{ij} , namely the possibility of decay from heavier to lighter dark-matter components. Once again, our starting points are the operators in Eqs. (1) and (2) which describe the microscopic (short-distance) interactions between our dark-sector particles χ_i and Standard-Model quarks. However, because we are considering dark-sector mass splittings of size $\Delta m_{12} \lesssim \mathcal{O}(\text{MeV})$, our study of the dark-matter decay induced by the operators in Eqs. (1) and (2) must instead be performed within the framework of a low-energy *macroscopic* effective field theory in which the physics of Eqs. (1) and (2) is recast in terms of interactions between

our dark-sector particles and the lightest color-neutral states in the visible sector.

In order to transition between these two descriptions, we can use the formalism of chiral perturbation theory [14] based on the low-energy $SU(2)_L \times SU(2)_R \times U(1)_V$ flavor symmetry group of the light (u, d) quarks [15]. This technique allows us to systematically generate a complete set of operators which capture the exact symmetry structure of our underlying microscopic Lagrangian, up to unknown (but ultimately measurable) coefficients $\tilde{\lambda}_i \sim \mathcal{O}(1)$. The details behind this calculation will be discussed more fully in Ref. [7]. The upshot, however, is that the scalar interaction in Eq. (1) gives rise to an effective Lagrangian of the form [16]

$$\begin{aligned} \mathcal{L}_{\text{eff}}^{(S)} = & -\frac{B_0^2(m_u - m_d)\tilde{\lambda}_1 c^{(S)}}{8\pi^2\Lambda^2} \bar{\chi}_2\chi_1 \\ & + \frac{B_0\alpha_{\text{EM}}\tilde{\lambda}_2 c^{(S)}}{4\pi\Lambda_C^2\Lambda^2} (\bar{\chi}_2\chi_1)F_{\mu\nu}F^{\mu\nu} + \dots, \end{aligned} \quad (7)$$

where $B_0 \equiv m_\pi^2/(m_u + m_d)$ and where Λ_C denotes the confinement scale $\Lambda_C \equiv 4\pi f_\pi/\sqrt{N_f}$, with $f_\pi \approx 93$ MeV and $N_f = 2$. Likewise, the axial-vector interaction in Eq. (2) gives rise to an effective Lagrangian of the form [16]

$$\begin{aligned} \mathcal{L}_{\text{eff}}^{(A)} = & -\frac{c^{(A)}\Lambda_C}{\sqrt{2}\pi\Lambda^2} \left[1 + \frac{m_\pi^2}{2\Lambda_C^2}\tilde{\lambda}_3 \right] (\bar{\chi}_2\gamma^\mu\gamma^5\chi_1)(\partial_\mu\pi^0) \\ & + \frac{\alpha_{\text{EM}}\tilde{\lambda}_4 c^{(A)}}{4\pi\Lambda_C^2\Lambda^2} (\bar{\chi}_2\gamma^\mu\gamma^5\chi_1)\partial_\mu(F_{\nu\rho}\tilde{F}^{\nu\rho}) + \dots \end{aligned} \quad (8)$$

We stress, however, that there are numerous subtleties involved in extracting these terms from the full chiral perturbation theory formalism. These will be discussed more fully in Ref. [7].

Somewhat surprisingly, the first term of Eq. (7) is not an interaction term, but rather an off-diagonal contribution to the mass matrix of the individual dark-sector components! At first glance, this might seem to suggest that the mass eigenstates of the dark sector are not given by the individual $\chi_{1,2}$ components with which we started, but rather by some new linear combinations of these states. However, our original supposition has always been that χ_1 and χ_2 are our physical mass eigenstates with masses m_1 and m_2 respectively — even in the confined phase of QCD within which we have been operating throughout this paper — and we know that the mass eigenstates of our theory should not change when we reshuffle our strongly interacting degrees of freedom from quarks to color-neutral hadrons. Thus, the contribution from this extra mass term within Eq. (7) must ultimately be cancelled by other additional mass terms (*e.g.*, coming from ultraviolet physics and/or other hadronic effects) so as to reproduce the mass eigenstates with which we started. That said, we might worry whether this cancellation might involve a significant degree of fine-tuning. However, it is easy to verify that this is not the

case throughout the region of parameter space in which we are primarily interested — *i.e.*, that within which $\Delta m_{12} \gtrsim \mathcal{O}(\text{keV})$ and $\Lambda \gtrsim \mathcal{O}(10 \text{ GeV})$. Indeed, within this region of parameter space, the degree of mixing associated with the mass matrix within Eq. (7) is negligible compared to Δm_{12} .

We therefore conclude that the mass term appearing within Eq. (7) is relatively unimportant for the present analysis in which we are focusing exclusively on dark-matter phenomenology within the confined phase of QCD. However, it is perhaps nevertheless worth remarking that terms of this sort can potentially play an important role in dark-matter *cosmology*, especially if the universe experiences a post-inflationary phase with a sufficiently high reheating temperature $T > \Lambda_{\text{QCD}}$. At such temperatures, the dark-sector mass matrix could in principle differ from its present-day form in a non-trivial manner. The process of confinement itself might then actually *induce* a re-diagonalization of the dark-sector mass eigenstates as part of the QCD phase transition, precisely through the appearance of terms such as those in Eq. (7). As a result, the mass eigenstates of the dark sector might not be the same before and after the QCD phase transition. In general, this is a novel effect which arises only for multi-component dark sectors. However, this effect can have a wealth of important theoretical and phenomenological implications, especially for dark-sector components χ_i and χ_j whose mass splittings Δm_{ij} are extremely small. These effects will be discussed further in Ref. [7].

The remaining terms in Eqs. (7) and (8) are *bona fide* interaction terms. As we see, they come in two types: contact operators (ultimately obtained from integrating out heavy hadronic degrees of freedom) which directly couple our dark-sector components χ_i to photons, and operators which couple our dark-sector components to off-shell pions (which then subsequently decay to two photons). These two sets of operators are illustrated in Fig. 3. Together, however, these operators allow us to calculate the widths for the decays $\chi_2 \rightarrow \chi_1 \gamma \gamma$ through either the scalar or the axial-vector interaction. For $\Delta m_{12} \ll m_{1,2}$, we obtain

$$\begin{aligned} \Gamma_{\gamma\gamma}^{(S)} &\approx \frac{B_0^2 \alpha_{\text{EM}}^2 \tilde{\lambda}_2^2 [c^{(S)}]^2}{8(105\pi^5) \Lambda_C^4 \Lambda^4} (\Delta m_{12})^7, \\ \Gamma_{\gamma\gamma}^{(A)} &\approx \frac{\alpha_{\text{EM}}^2 [c^{(A)}]^2}{8(315\pi^5) \Lambda_C^4 \Lambda^4} \left[\tilde{\lambda}_3 - \tilde{\lambda}_4 + \frac{2\Lambda_C^2}{m_\pi^2} \right]^2 (\Delta m_{12})^9. \end{aligned} \quad (9)$$

These decay rates may then be compared against existing bounds on observed photon fluxes in order to constrain our fundamental parameters $(c/\Lambda^2, \Delta m_{12})$ for different values of m_2 . In particular, assuming an NFW profile for the dark-matter distribution [17], we use the PPPC4DMID software package [18] to determine the diffuse galactic and extragalactic contributions to the differential photon flux arising from dark-matter decay, and

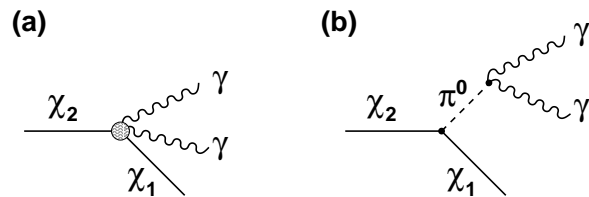


FIG. 3: Dominant dark-matter decay processes at energies $E \lesssim \mathcal{O}(10^2) \text{ keV}$. (a) Dark-matter decay produces two photons through an effective contact operator induced in the chiral perturbation theory by integrating out heavy hadrons. This process is the dominant contributor in the case of the microscopic (quark-level) scalar interaction in Eq. (1). (b) Dark-matter decay produces two photons via off-shell neutral-pion exchange. Both this process and the process in (a) are the dominant contributors in the case of the microscopic (quark-level) axial-vector interaction in Eq. (2).

require that the predicted photon count not exceed that measured in any bin at the 2σ confidence level. In this context we remark that decays to final states involving neutrinos are also kinematically allowed. However, the contributions to the total widths from such decays are negligible compared with the above, and are thus neglected.

Results.— Combining the constraints from each of the dark-matter directions discussed above, we can now map out the current bounds on the operators in Eqs. (1) and (2) in the $(c/\Lambda^2, \Delta m_{12})$ parameter space for different values of m_2 . Our results are shown in Fig. 4 for $m_2 = \{10, 100, 1000\} \text{ GeV}$, with $c^{(S)} = c^{(A)} = 1/\sqrt{2}$ and $\tilde{\lambda}_i = 1$ chosen as fixed reference values.

In Fig. 4, the pink regions are excluded by bounds on inelastic scattering from direct-detection experiments (LUX [8] and COUPP-4 [9] for the scalar and axial-vector cases, respectively), while the green contour indicates the projected future reach of the LZ 7.2-ton detector [19] in the scalar case and the PICO-250L experiment [20] in the axial-vector case. Likewise, the vertical blue and cyan contours respectively correspond to LHC constraints on asymmetric collider production from monojet [10, 11] and hadronically-decaying mono- W/Z [12] searches. The collider analysis was performed by generating signal events using the MadGraph 5 [21], Pythia 6.4 [22], and Delphes 2.0.5 [23] software packages, and comparing to the number of background events reported in Refs. [10–12] in order to determine the region excluded at 90% confidence level. Note that there is a $\sim 40\%$ systematic uncertainty in the number of signal events, attributable to uncertainties in the correct treatment of soft QCD and hadronic physics; this uncertainty can affect the bounds on Λ by $\sim 10\%$. In this connection we also remind the reader that these collider-based bounds should be interpreted at best only heuristically if the operators in Eqs. (1) and (2) are generated by inte-

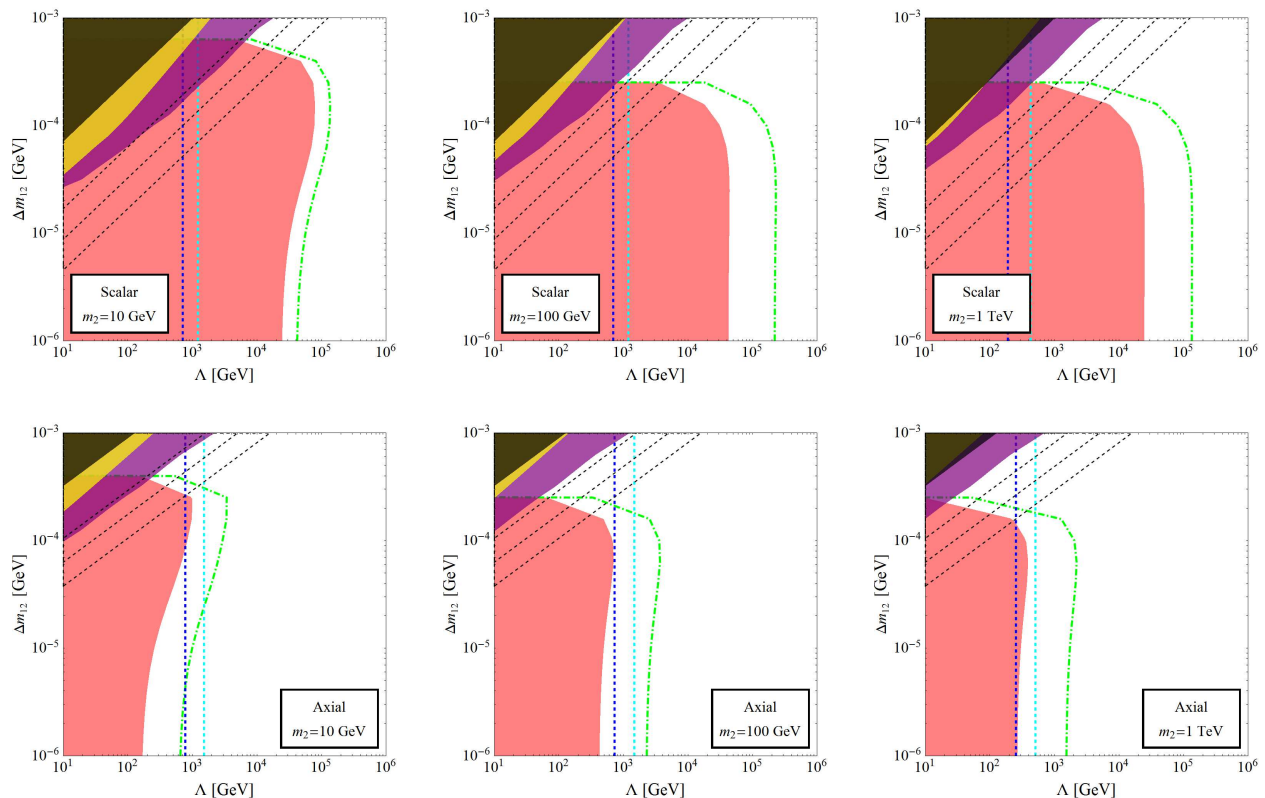


FIG. 4: Complementary bounds on the scalar operator in Eq. (1) and axial-vector operator in Eq. (2), plotted within the associated $(\Lambda, \Delta m_{12})$ parameter spaces for $m_2 = \{10, 100, 1000\}$ GeV and $c^{(S)} = c^{(A)} = 1/\sqrt{2}$. Bounds from inelastic-scattering direct-detection experiments (pink exclusion regions), asymmetric collider production (blue and cyan vertical lines), and dark-matter decay constraints (yellow and purple exclusion regions) are shown, as discussed in the text; the green dashed lines denote the reaches of possible future direct-detection experiments, while the black dashed lines indicate dark-matter decay lifetime contours, as discussed in the text, and the solid black triangular regions in each panel are excluded by metastability constraints. Remarkably, the constraints from dark-matter decay dominate in exactly those regions with relatively large Δm_{12} that lie beyond the reach of current and future direct-detection experiments, thereby illustrating the new sorts of complementarities that are possible for such multi-component dark sectors.

grating out light mediators or by other new physics which renders $\Lambda \lesssim \mathcal{O}(\text{TeV})$. The yellow and purple shaded regions are excluded by constraints on dark-matter decay from the total diffuse X-ray background measurements of HEAO-1 [24] and INTEGRAL [25], respectively, as these are the experiments which probe the particular energy region of the photon spectrum which is most relevant for the Δm_{12} range with which we are most concerned. Finally, the diagonal dashed black lines from left to right respectively indicate contours corresponding to dark-matter lifetimes $\tau_2 = 10^{22}$ s, 10^{24} s, and 10^{26} s. By contrast, the solid black triangular regions are excluded by metastability constraints which require that $\tau_2 \gtrsim t_{\text{now}}$, where $t_{\text{now}} \approx 4.35 \times 10^{17}$ s is the current age of the universe. Note that in all cases, these metastability bounds for χ_2 are superseded by the results from dark-matter decay. Mechanisms for having such long-lived dark-matter components can be found, for example, in Ref. [26].

There are many important features contained within

the plots in Fig. 4. Since Δm_{12} effectively quantifies departures from the standard single-component story, we shall discuss these features “from bottom up”, in order of increasing Δm_{12} .

First, for $\Delta m_{12} \lesssim \mathcal{O}(10 \text{ keV})$, we see that all of the features within these plots are virtually insensitive to Δm_{12} and effectively reproduce the physics of a traditional single-component dark sector with mass m_2 . This behavior is certainly expected in the $\Delta m_{12} \rightarrow 0$ limit, and as a check we see that the middle panels of Fig. 4 correctly reproduce the results in Eqs. (4) and (5) in this limit. However, we now observe that these results persist all the way up to $\Delta m_{12} \lesssim \mathcal{O}(10 \text{ keV})$, thereby forming an “asymptotic” region in which the physics remains largely Δm_{12} -independent. Thus, for the operators in Eq. (1) and (2), we see that it is only for $\Delta m_{12} \gtrsim \mathcal{O}(10 \text{ keV})$ that the effects of dark-sector non-minimality become evident.

Second, for $\Delta m_{12} \approx \mathcal{O}(10\text{--}100 \text{ keV})$, we see that the bounds from direct-detection experiments actually

strengthen somewhat and begin to extend towards larger values of Λ . As we see from Fig. 4, this behavior is more pronounced for the axial-vector interaction than the scalar interaction and for smaller values of m_2 rather than larger. This strengthening can more than double the values of Λ probed by such experiments, and is particularly important because it has the power to alter the identity of the specific dark-matter detection method which provides the leading constraint on the scale Λ as a function of Δm_{12} . For example, in the case of the axial-vector interaction with $m_2 = 10$ GeV (corresponding to the lower left panel of Fig. 4), we see that the monojet and mono- W/Z collider processes provide the strongest constraints for $\Delta m_{12} \lesssim \mathcal{O}(10 \text{ keV})$, but that the bounds from the direct-detection processes become increasingly strong with growing Δm_{12} , ultimately matching and perhaps even superseding the monojet collider bounds for $\Delta m_{12} \approx \mathcal{O}(100 \text{ keV})$. This strengthening of the direct-detection bounds as a function of increasing Δm_{12} is a direct consequence of the inelastic nature of the scattering process involved.

Third, moving towards even larger values $\Delta m_{12} \approx \mathcal{O}(100 - 1000 \text{ keV})$, we see that the plots in Fig. 4 now reveal a dramatic feature: a “ceiling” for Δm_{12} beyond which direct-detection experiments cease to provide any bounds at all and become virtually insensitive to the underlying dark-sector physics! This is also ultimately a consequence of the unique kinematics associated with inelastic down-scattering. As discussed above, for down-scattering there is a lower limit of nuclear recoil energies $E_R^{(\text{min})}$ below which the differential scattering rate dE_R/dR becomes negligible (see Fig. 2). This lower limit generally increases with increasing Δm_{ij} and is not too far below E_R^* for the non-relativistic dark-matter velocities concerned. However, a given dark-matter direct-detection experiment is typically designed to probe only a particular window of recoil energies. While the precise window of recoil energies depends on the type of experiment and the cuts imposed as part of the data analysis, this window typically falls within the range $1 \text{ keV} \lesssim E_R \lesssim 100 \text{ keV}$, as discussed above. Scattering events with recoil energies outside this range do not contribute to the measured signal-event rate. As a result, there exists a critical value of Δm_{12} beyond which the corresponding down-scattering events have a minimum recoil energy $E_R^{(\text{min})}$ exceeding 100 keV, thereby escaping detection.

Fourth, moving towards even larger values $\Delta m_{12} \lesssim \mathcal{O}(\text{MeV})$, we see from Fig. 4 that the physics is now dominated by the constraints from dark-matter decay. Indeed, these constraints become significantly more stringent as Δm_{12} increases, with the maximum reach Λ_{max} scaling approximately as $(\Delta m_{12})^{7/4}$ and $(\Delta m_{12})^{9/4}$ for the scalar and axial-vector interactions, respectively. It should also be noted that these decay

constraints even have a subtle dependence on m_2 . Indeed, although the decay widths in Eq. (9) are independent of m_2 for $\Delta m_{12} \ll m_2$, we see that m_2 nevertheless enters the calculation of the total fluxes of the remnants of such decays through its appearance in the χ_2 number density $n_2 \approx \Omega_2/m_2$, where Ω_2 is the dark-matter abundance which we have assumed fixed at $\Omega_2 = \Omega_{\text{CDM}} \approx 0.26$. There are, of course, further m_2 -dependent corrections to both the decay widths and the injection spectra which emerge once we go beyond the $\Delta m_{12} \ll m_2$ approximation; these have been included in the plots shown in Fig. 4, but otherwise have a negligible effect on our results.

Finally, although we have restricted our focus in this paper to the region $\Delta m_{12} \lesssim \mathcal{O}(\text{MeV})$, it is interesting to contemplate what occurs for even greater Δm_{12} . For $\Delta m_{12} \gtrsim \mathcal{O}(\text{MeV})$, additional decay channels for χ_2 open up in which electron/positron pairs are the end products. This only increases the decay widths for χ_2 , thereby strengthening the Λ -reach of the decay-related bounds even further. For even greater values of Δm_{12} , these decay widths increase still further as additional decay channels become kinematically accessible. Ultimately, however, Δm_{12} reaches a point at which even the metastability that underlies our assumption of a non-zero present-day abundance for χ_2 is threatened. In this connection, it is important to note that this does not render such multi-component theories inconsistent; indeed, for multi-component theories it has been demonstrated that dark-matter stability is not a fundamental requirement — all that is required is a balancing of their individual component lifetimes against their cosmological abundances [27]. However, this shift does alter the initial assumptions that enter into the types of calculations we have performed in this paper. It would nevertheless be interesting to extend this type of complementarity analysis to the constraints emerging from such a scenario.

The plots in Fig. 4 thus provide dramatic illustration of the new complementarities that emerge within the context of non-minimal dark sectors. Together, the bounds from asymmetric collider-production processes, inelastic-scattering processes, and dark-matter decay processes not only help to increase the *coverage* of the relevant parameter spaces of these models but also provide useful *correlations* between these processes in those regions of parameter space in which these constraints overlap. For example, it is somewhat remarkable that the constraints from dark-matter decay emerge and dominate in exactly those regions that lie just beyond the Δm_{12} “ceiling” that caps the reach of current and future direct-detection experiments. This result is especially gratifying, given that any operators and initial conditions which give rise to inelastic down-scattering direct-detection signals in a multi-component context must also necessarily give rise to dark-matter decays. Perhaps even more interestingly, we see that in the axial-vector case there

even exists a small window within the “cross-over” region $\Delta m_{12} \approx 500$ keV (sandwiched between the bounds from direct-detection and dark-matter decay processes) in which it is the mono- W/Z collider bounds which provide the strongest current constraints. Taken together, this non-trivial structure is testament to the richness of the complementarities that emerge when Δm_{12} is lifted beyond the $\Delta m_{12} = 0$ axis to which the traditional complementarities that govern the physics of single-component dark sectors are restricted.

Conclusions.— The idea of complementarity has long infused our thinking about the hunt for dark matter, but most work on this subject has focused on the case of single-component dark sectors. In this paper, by contrast, we have considered the case of a multi-component dark sector, and demonstrated that there exist entirely new directions for complementarity which are absent in single-component theories. In particular, we demonstrated that the important class of interactions involving two dark components and two visible components can simultaneously contribute to *inelastic* scattering at direct-detection experiments, *asymmetric* dark-matter production at colliders, and indirect-detection signals due to dark-matter *decay*. Indeed, the latter phenomenon is completely absent for such interactions within single-component dark-matter theories, and thus represents an entirely new direction for dark-matter complementarity that emerges only within the multi-component context.

We have also demonstrated the power of these complementarity relations by considering two particular examples of such interactions, one based on a scalar (spin-independent) interaction and the other based on an axial-vector (spin-dependent) interaction. In some regimes involving large couplings or small cutoff scales Λ , we found that there is significant overlap between the regions excluded by direct- and indirect-detection limits. Taken together, these complementary probes of the dark sector combine to provide complete coverage of the relevant parameter space in this regime. By contrast, in other regimes involving smaller couplings and/or larger cutoff scales Λ , a small slice of parameter space opens up for which the dark sector escapes detection.

The existence of such regions of parameter space provides extra motivation for the development of new experimental detection strategies which are specifically targeted towards physics in these regions. For example, it would be interesting to explore how improvements in, *e.g.*, the angular resolution of future X-ray telescopes could improve the reach of indirect-detection experiments within the parameter space of non-minimal dark sectors. Likewise, designing a calibration for incorporating higher-energy nuclear recoils into threshold-detector analyses of the data from direct-detection experiments also represents a possible future method of “filling in the gap” between the bounds from direct-detection experiments and those from dark-matter decay. Finally, we

note that direct-detection experiments using heavier target nuclei would in principle be capable of probing regions of parameter space with larger Δm_{12} .

Needless to say, there are also many future theoretical directions that can be pursued. One is to consider a wider class of operators beyond those considered here [7]. The case of pseudoscalar operators, in particular, may be of particular interest due to the existence of previously unnoticed effects which are capable of overcoming the velocity suppression that would otherwise affect the corresponding direct-detection processes [28].

Another possible future direction is to consider the physics that might result from different configurations of initial abundances Ω_1 and Ω_2 . In this paper we have focused on the case with $\Omega_1 \approx 0$ and $\Omega_2 \approx \Omega_{\text{CDM}}$, since this configuration leads to the strongest possible bounds for both direct- and indirect-detection experiments. Although this configuration may initially seem somewhat unnatural or fine-tuned, one can imagine that it is realized in cosmological scenarios in which the production of heavier dark-matter states is overwhelmingly favored relative to that of lighter dark-matter states, or in which the bulk of the dark matter is somehow excited into the higher-mass χ_2 state after production. It is nevertheless of interest to explore the phenomenology associated with more general configurations, particularly those such as $\Omega_1 \approx \Omega_2 \approx \Omega_{\text{CDM}}/2$ which might be imagined as emerging from a straightforward thermal-production mechanism. Obviously, any scenario with non-zero Ω_1 will generally involve contributions from processes such as up-scattering (in addition to down-scattering) and dark-matter co-annihilation (in addition to dark-matter decay). However, it often turns out that the constraints from both of these processes are subleading within their respective classes (direct- and indirect-detection signals, respectively); indeed, co-annihilation will not even occur in scenarios (such as those associated with asymmetric dark matter [29]) in which the abundance of dark anti-matter does not match that of dark matter and is effectively zero at present times. Thus, in such cases, the primary effect of shifting some abundance $\Delta\Omega$ from Ω_2 to Ω_1 (thereby resulting in $\Omega'_2 \equiv \Omega_2 - \Delta\Omega$) is merely to weaken the constraints from down-scattering and dark-matter decay by the factor $\Omega'_2/\Omega_2 \equiv 1 - \Delta\Omega/\Omega_2$. On logarithmic plots such as those in Fig. 4, such $\mathcal{O}(1)$ rescaling factors are barely noticeable. Such effects will be discussed further in Ref. [7].

A third possible future direction is to realize that even though we have restricted our attention to operators such as those in Eqs. (1) and (2) which only couple χ_i to χ_j with $i \neq j$, a more general theory involving four-fermi operators of this sort is likely to include the “diagonal” $i = j$ operators as well. We did not study such “diagonal” operators in this paper because such operators appear even in single-component theories of dark matter; they therefore do not represent the new physics we

wished to explore. However, in a general theory, “diagonal” and “non-diagonal” operators are likely to appear together. In such cases, as discussed in the Introduction, both elastic and inelastic scattering events can simultaneously occur within a given direct-detection experiment, while dark-matter production at colliders can have both symmetric and asymmetric channels and the cosmic-ray fluxes relevant for indirect-detection experiments can potentially include the products of dark-matter self-annihilation as well as co-annihilation between different dark-matter species and dark-matter decay. It will clearly be of interest to study the experimental complementarity bounds that emerge when all of these processes are included simultaneously. In particular, we note that it might even be possible to establish *correlations* between the signals from dark-matter decay and dark-matter (co-)annihilation in such a way as to potentially distinguish these signals from those which might be produced through other, unrelated astrophysical phenomena such as pulsars.

Finally, a fourth possible direction for future study is to recognize that a non-minimal dark sector may have a relatively large number of individual components which could potentially give rise to collective effects that transcend the two-component effects studied here. A dramatic example of this occurs within the so-called “Dynamical Dark Matter” (DDM) framework [27]; this framework gives rise to unexpected signatures not only for collider experiments [30] but also for direct-detection experiments [31] and indirect-detection experiments [32]. Studying the full parameter space of such models, especially from a complementarity perspective, should be an interesting exercise [7].

This work was supported in part by the U.S. Department of Energy under Grant DE-FG02-13ER-41976 (KRD), by the U.S. National Science Foundation under CAREER Award PHY-1250573 (JK), by the Natural Sciences and Engineering Research Council of Canada (BT), and by U.S. Department of Energy under Grant DE-FG02-13ER-42024 (DY). The opinions and conclusions expressed herein are those of the authors, and do not represent any funding agency. We are happy to thank Z. Chacko and U. van Kolck for discussions.

[1] For reviews, see, *e.g.*:

G. Jungman, M. Kamionkowski and K. Griest, Phys. Rept. **267**, 195 (1996) [arXiv:hep-ph/9506380];
 J. D. Lewin and P. F. Smith, Astropart. Phys. **6**, 87 (1996);
 D. Hooper, [arXiv:0901.4090 [hep-ph]];
 N. Weiner, “Dark Matter Theory,” video of lectures given at TASI 2009, http://physicslearning2.colorado.edu/tasi/tasi_2009/tasi_2009.htm;

- J. L. Feng, Ann. Rev. Astron. Astrophys. **48**, 495 (2010) [arXiv:1003.0904 [astro-ph.CO]];
 R. W. Schnee, arXiv:1101.5205 [astro-ph.CO].
- [2] S. Arrenberg *et al.*, arXiv:1310.8621 [hep-ph].
- [3] T. Han and R. Hempfling, Phys. Lett. **B415**, 161 (1997) [arXiv:hep-ph/9708264];
 L. J. Hall, T. Moroi and H. Murayama, Phys. Lett. **B424**, 305 (1998) [arXiv:hep-ph/9712515];
 D. Tucker-Smith and N. Weiner, Phys. Rev. D **64**, 043502 (2001) [arXiv:hep-ph/0101138]; Phys. Rev. D **72**, 063509 (2005) [hep-ph/0402065].
- [4] F. Chen, J. M. Cline and A. R. Frey, Phys. Rev. D **79**, 063530 (2009) [arXiv:0901.4327 [hep-ph]];
 D. P. Finkbeiner, T. R. Slatyer, N. Weiner and I. Yavin, JCAP **0909**, 037 (2009) [arXiv:0903.1037 [hep-ph]];
 B. Batell, M. Pospelov and A. Ritz, Phys. Rev. D **79**, 115019 (2009) [arXiv:0903.3396 [hep-ph]];
 P. W. Graham, R. Harnik, S. Rajendran and P. Saraswat, Phys. Rev. D **82**, 063512 (2010) [arXiv:1004.0937 [hep-ph]].
- [5] D. P. Finkbeiner and N. Weiner, Phys. Rev. D **76**, 083519 (2007) [astro-ph/0702587];
 J. M. Cline, A. R. Frey and F. Chen, Phys. Rev. D **83**, 083511 (2011) [arXiv:1008.1784 [hep-ph]];
 N. F. Bell, A. J. Galea and R. R. Volkas, Phys. Rev. D **83**, 063504 (2011) [arXiv:1012.0067 [hep-ph]].
- [6] M. Pospelov and A. Ritz, Phys. Rev. D **84**, 113001 (2011) [arXiv:1109.4872 [hep-ph]];
 A. Drozd, B. Grzadkowski and J. Wudka, JHEP **1204**, 006 (2012) [arXiv:1112.2582 [hep-ph]];
 C. Cheung and Y. Nomura, Phys. Rev. D **86**, 015004 (2012) [arXiv:1112.3043 [hep-ph]];
 Y. Bai, P. Draper and J. Shelton, JHEP **1207**, 192 (2012) [arXiv:1112.4496 [hep-ph]];
 S. Bhattacharya, A. Drozd, B. Grzadkowski and J. Wudka, JHEP **1310**, 158 (2013) [arXiv:1309.2986 [hep-ph]];
 J. Wang, Phys. Rev. D **89**, 093019 (2014) [arXiv:1311.3442 [hep-ph]].
- [7] K. R. Dienes, J. Kumar, B. Thomas and D. Yaylali, to appear.
- [8] D. S. Akerib *et al.* [LUX Collaboration], Phys. Rev. Lett. **112**, 091303 (2014) [arXiv:1310.8214 [astro-ph.CO]].
- [9] E. Behnke *et al.* [COUPP Collaboration], Phys. Rev. D **86**, 052001 (2012) [arXiv:1204.3094 [astro-ph.CO]].
- [10] G. Aad *et al.* [ATLAS Collaboration], JHEP **1304**, 075 (2013) [arXiv:1210.4491 [hep-ex]];
 ATLAS Collaboration, ATLAS-CONF-2012-147.
- [11] S. Chatrchyan *et al.* [CMS Collaboration], JHEP **1209**, 094 (2012) [arXiv:1206.5663 [hep-ex]];
 CMS Collaboration, CMS-PAS-EXO-12-048.
- [12] G. Aad *et al.* [ATLAS Collaboration], Phys. Rev. Lett. **112**, 041802 (2014) [arXiv:1309.4017 [hep-ex]];
 arXiv:1404.0051 [hep-ex].
- [13] N. Anand, A. L. Fitzpatrick and W. C. Haxton, arXiv:1308.6288 [hep-ph].
- [14] For reviews, see, *e.g.*:
 U. G. Meissner, Rept. Prog. Phys. **56**, 903 (1993) [hep-ph/9302247];
 G. Ecker, Prog. Part. Nucl. Phys. **35**, 1 (1995) [hep-ph/9501357];
 A. Pich, Rept. Prog. Phys. **58**, 563 (1995) [hep-ph/9502366];
 G. Colangelo and G. Isidori, hep-ph/0101264;

- S. Scherer, *Adv. Nucl. Phys.* **27**, 277 (2003) [hep-ph/0210398].
- [15] J. Gasser and H. Leutwyler, *Annals Phys.* **158**, 142 (1984);
H. Leutwyler, *Annals Phys.* **235**, 165 (1994) [hep-ph/9311274];
R. Kaiser, *Phys. Rev. D* **63**, 076010 (2001) [hep-ph/0011377].
- [16] H. W. Fearing and S. Scherer, *Phys. Rev. D* **53**, 315 (1996) [hep-ph/9408346];
J. Bijnens, G. Colangelo and G. Ecker, *JHEP* **9902**, 020 (1999) [hep-ph/9902437];
T. Ebertshauser, H. W. Fearing and S. Scherer, *Phys. Rev. D* **65**, 054033 (2002) [hep-ph/0110261];
J. Bijnens, L. Girlanda and P. Talavera, *Eur. Phys. J. C* **23**, 539 (2002) [hep-ph/0110400].
- [17] J. F. Navarro, C. S. Frenk and S. D. M. White, *Astrophys. J.* **462**, 563 (1996) [astro-ph/9508025].
- [18] M. Cirelli *et al.*, *JCAP* **1103**, 051 (2011) [Erratum-ibid. **1210**, E01 (2012)] [arXiv:1012.4515 [hep-ph]].
- [19] R. Gaiatskell *et al.*, <http://dmtools.brown.edu:8080>;
D. C. Malling *et al.*, arXiv:1110.0103 [astro-ph.IM].
- [20] R. Neilson, talk given at Aspen 2013, <http://http://indico.cern.ch/event/197862/session/3/contribution/69/material/slides/0.pdf>.
- [21] J. Alwall, M. Herquet, F. Maltoni, O. Mattelaer and T. Stelzer, *JHEP* **1106**, 128 (2011) [arXiv:1106.0522 [hep-ph]].
- [22] T. Sjostrand, S. Mrenna and P. Z. Skands, *JHEP* **0605**, 026 (2006) [hep-ph/0603175].
- [23] S. Ovnyn, X. Rouby and V. Lemaitre, arXiv:0903.2225 [hep-ph].
- [24] D. E. Gruber, J. L. Matteson, L. E. Peterson and G. V. Jung, *Ap. J.* **520**, 124 (1999) [astro-ph/9903492].
- [25] L. Bouchet, E. Jourdain, J. P. Roques, A. Strong, R. Diehl, F. Lebrun and R. Terrier, *Ap. J.* **679**, 1315 (2008) [arXiv:0801.2086 [astro-ph]].
- [26] M. Fairbairn and J. Zupan, *JCAP* **0907**, 001 (2009) [arXiv:0810.4147];
H. Fukuoka, J. Kubo and D. Suematsu, *Phys. Lett.* **B678**, 401 (2009) [arXiv:0905.2847].
- [27] K. R. Dienes and B. Thomas, *Phys. Rev. D* **85**, 083523 (2012) [arXiv:1106.4546 [hep-ph]]; *Phys. Rev. D* **85**, 083524 (2012) [arXiv:1107.0721 [hep-ph]]; *Phys. Rev. D* **86**, 055013 (2012) [arXiv:1203.1923 [hep-ph]].
- [28] K. R. Dienes, J. Kumar, B. Thomas and D. Yaylali, *Phys. Rev. D* **90**, 015012 (2014) [arXiv:1312.7772 [hep-ph]].
- [29] S. Nussinov, *Phys. Lett. B* **165**, 55 (1985);
G. B. Gelmini, L. J. Hall and M. J. Lin, *Nucl. Phys. B* **281**, 726 (1987);
S. M. Barr, R. S. Chivukula and E. Farhi, *Phys. Lett. B* **241**, 387 (1990);
S. M. Barr, *Phys. Rev. D* **44**, 3062 (1991);
D. B. Kaplan, *Phys. Rev. Lett.* **68**, 741 (1992);
S. B. Gudnason, C. Kouvaris and F. Sannino, *Phys. Rev. D* **73**, 115003 (2006) [hep-ph/0603014]; *Phys. Rev. D* **74**, 095008 (2006) [hep-ph/0608055];
R. Kitano and I. Low, *Phys. Rev. D* **71**, 023510 (2005) [hep-ph/0411133]; hep-ph/0503112;
D. E. Kaplan, M. A. Luty and K. M. Zurek, *Phys. Rev. D* **79**, 115016 (2009) [arXiv:0901.4117 [hep-ph]].
- [30] K. R. Dienes, S. Su and B. Thomas, *Phys. Rev. D* **86**, 054008 (2012) [arXiv:1204.4183 [hep-ph]].
- [31] K. R. Dienes, J. Kumar and B. Thomas, *Phys. Rev. D* **86**, 055016 (2012) [arXiv:1208.0336 [hep-ph]].
- [32] K. R. Dienes, J. Kumar and B. Thomas, *Phys. Rev. D* **88**, 103509 (2013) [arXiv:1306.2959 [hep-ph]].